

Configuration Synthesis for Fully Restrained 7-Cable-Driven Manipulators

Regular Paper

Xiaoqiang Tang^{1,*}, Lewei Tang¹, Jinsong Wang¹ and Dengfeng Sun²

¹ The State Key Laboratory of Tribology, Department of Precision Instruments and Mechanology, Tsinghua University, Beijing, P.R. of China

² School of Aeronautics and Astronautics Engineering, Purdue University, West Lafayette, IN

* Corresponding author E-mail: tang-xq@mail.tsinghua.edu.cn

Received 7 May 2012; Accepted 6 Aug 2012

DOI: 10.5772/52147

© 2012 Tang et al.; licensee InTech. This is an open access article distributed under the terms of the Creative Commons Attribution License (<http://creativecommons.org/licenses/by/3.0>), which permits unrestricted use, distribution, and reproduction in any medium, provided the original work is properly cited.

Abstract Cable distribution plays a vital role in Cable Driven Parallel Manipulators (CDPMs) regarding tension and workspace quality, especially in fully restrained CDPMs. This paper focuses on three typical configurations of fully restrained CDPMs with 7 cables in order to introduce an approach for configuration synthesis. Firstly, the kinematic models of three types of CDPMs with 7 cables are set up. Then, in order to evaluate workspace quality, two new indices are proposed by using tensions along each cable, which are the All Cable Tension Distribution Index (ACTDI) and Global Tension Distribution Index (GTDI). Next, the three types of CDPMs with 7 cables are analysed with the two indices. At the end, according to different performance requirements, the configurations of cable distribution are discussed and selected.

Keywords Cable driven parallel manipulator, Configuration synthesis, Workspace quality, Tension distribution

1. Introduction

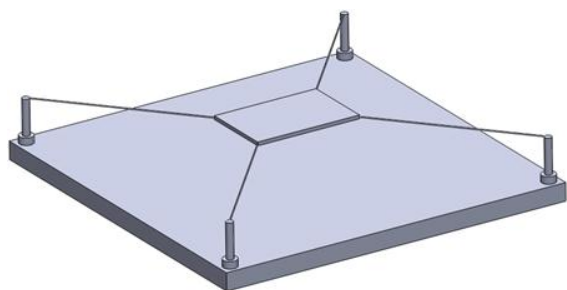
Cable Driven Parallel Manipulators (CDPMs) are a set of parallel manipulators driven/suspended by several

cables/wires. Compared with parallel manipulators joined by rigid linkages, CDPMs reveal some promising practical advantages, such as larger workspace, lower inertia and higher payload ratio. Thus, aspects of CDPMs have been widely researched in the last twenty years including workspace[1,2,3], tension optimization [4,5], singularity[6,7]and control[8,9].

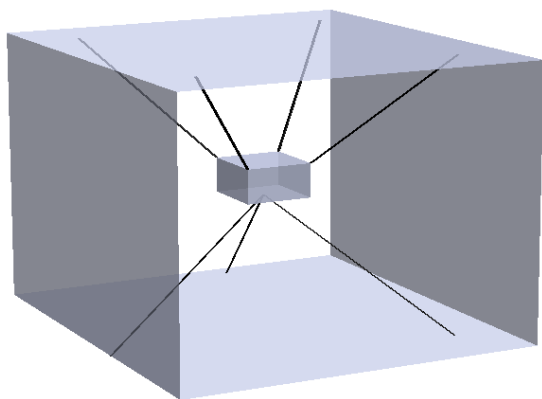
Some conclusions drawn are that the cables/wires can only be suspended because the flexibility of cables/wires makes themselves endure tension rather than pressure. Due to these features, many researchers have confirmed that m cables control $m-1$ DOFs (Fully Restrained CDPMs / Completely Restrained CDPMs) or less than $m-1$ DOFs (Redundant Restrained CDPMs)[2,6,7,8]. From the point of simplification, completely restrained CDPMs realize the manipulation of a moving platform with the least cables. Therefore, we need to solve the fundamental problem of the evaluation of the completely restrained CDPMs in different configurations. As for completely restrained CDPMs, they are divided into two classes: namely planar CDPMs and spatial CDPMs, illustrated in Fig. 1. In addition, the planar CDPM driven by 4 cables can obtain 3 DOFs (2 translation DOFs and 1 rotation DOF), this has been extensively investigated in

[5,7,10,11,12], and the spatial CDPM driven by 7 cables can control 6 DOFs instead [3]. By further research, the spatial CDPMs are respectively more sophisticated than the planar CDPMs because the schemes for distributing the cables in 3D space are larger in number. Disregarding of gravity, the distribution of cables can be summarized as 8 types. However, the 2 types with all the cables on one side cannot meet the force-close condition, and the other 6 types will only have 3 type workspaces for the workspace upside down with the same number. Generally, the joints on fixed platforms are uniformly distributed, while those on moving platform are attached altogether avoiding cable collision [3, 9,13,14]. Hence, the main distribution configurations of completely restrained CDPMs with 6 DOFs are listed in Table 1.

Generally, the essential problem of how to define the boundary of the workspace should be solved first. Moreover, the workspace determination can be subdivided into two categories, namely the workspace with a fixed orientation and the workspace with a fixed position. After obtaining the workspace, the second problem, of tension distribution should be considered in workspaces as a whole. Furthermore, spatial CDPMs in different configurations have their own features. In light of this, the evaluation of spatial CDPMs aims to compare and select the better kinds of configuration in constrained conditions.



(a) A planar CDPM



(b) A spatial CDPM

Figure 1. Completely Restrained CDPMs

Type	Configuration	Description
1-6		Higher Cables:1 Lower Cables:6
2-5		Higher Cables:2 Lower Cables:5
3-4		Higher Cables:3 Lower Cables:4

Table 1. Distribution Schemes

Based on current research on CDPMs workspace, the first problem mentioned above is the same as how to meet force-close condition with positive tensions. C. B. Pham analyses the planar CDPMs workspace with the null space method[1] and proposes a recursive dimension reduction algorithm with Gaussian elimination to study Redundant Restrained CDPMs workspace later[15]. X. Diao presents a method of verifying force-closure conditions for CDPMs[3]. D. Lau states a hybrid analytical-numerical approach to calculate the workspace in detail[16]. These approaches have been proved to be valid to map the workspace. Particularly, Darwin Lau compares the running time when solving the workspace determination problem. As for the second problem, C. B. Pham defines two indices by using the maximum and the minimum tensions to measure the workspace quality but ignores other tensions. In this paper, we deal with the evaluation of workspace quality of the spatially completely restrained CDPMs in different configurations with 7 cables using three indices.

This paper is organized as follows: The modelling principles of fully restrained CDPMs with 7 cables are presented in Section 2, where three typical configurations are put forward. Based on force-close conditions, tensions along with cables are analyzed in Section 3, which is followed by introducing a method to obtain the

workspace of CDPMs in Section 4. Then, three indices are addressed so as to evaluate the workspace quality in Section 5. Next, the workspace quality is discussed by ACTDI and GDTI in Section 6. Finally, the paper is summarized in Section 7.

2. Modelling principle

As listed in Table1, three kinds of completely restrained CDPMs are discussed in this paper. In total, there are three circular platforms in each type, namely the higher fixed platform, the lower fixed platform and the middle moving platform. The radii of these two fixed platforms are defined as R_H and R_L , the distance between these fixed platforms is h , and the radius of the middle moving platform is R_M as show in Table2. The higher cables connecting the higher fixed platform and the middle moving platform are attached together at the centre of the moving platform. The cables joining the higher fixed platform are distributed equally except for only one cable, which is bonded with the centre of the higher fixed platform. And the cables connecting the middle moving platform and the lower fixed platform are attached to three distributed linking joints on the middle moving platform, while the joints on the lower fixed platform are symmetrical. Additionally, the joints on the higher and lower fixed platforms are also axisymmetric. Therefore, three models are selected as the representatives of these configurations in Fig.2, and the position vectors are added in the Appendix.

Parameters	Value/mm
R_H	500
R_L	500
R_M	150
h	1000

Table 2. Modelling Parameters

3. Tension conditions

A typical completely restrained cable-driven parallel manipulator consists of two fixed platforms and a moving platform with several cables as in Table 1. The tensions in each cable should satisfy the force-close conditions, which are also known as the tension conditions.

3.1 Kinematical modelling

The kinematical models of fully restrained CDPMs with 7 cables are showed in Fig.2. The values of these modelling parameters are listed in Table 2. The global frame $\{G\}$ F_0 -XYZ is located at the centre of the lower fixed platform, while the local frame $\{P\}$ F_e -XYZ is attached to the geometric centre of the moving platform.

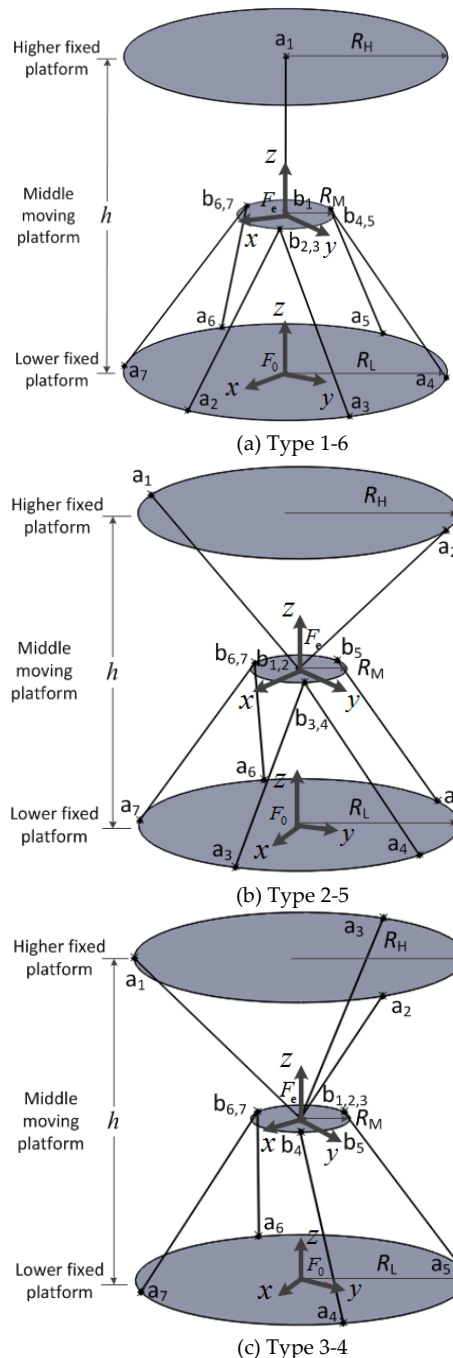


Figure 2. Kinematical models of CDPMs

3.2 Force and torque equilibriums

Given an arbitrary external wrench $({}^o\mathbf{f}, {}^o\mathbf{m})'$ on the moving platform, tension in the m cable can control $m-1$ DOFs CDPM, which must satisfy the force and torque equilibrium below:

$$\begin{aligned} \sum_{i=1}^m \mathbf{t}_i + {}^o\mathbf{f} &= 0 \\ \sum_{i=1}^m {}^e\mathbf{b}_i \times \mathbf{t}_i + {}^o\mathbf{m} &= 0 \end{aligned} \quad (1)$$

where \mathbf{t}_i ($i = 1, 2, \dots, m$) is the tension vector of i cable.

4. Workspace solving approach

It is clear that the position and orientation is in the workspace if the tensions of cables meet Eq. (1) with positive values. However, Eq. (1) is hard to solve thus defining the workspace of CDPMs is always difficult. Next, we propose a new approach to solve this problem by combing the force-close condition with the tension limitations.

Based on the definition of the completely restrained CDPMs, m DOFs of the moving platform need $m+1$ cables for control. Hence, Eq. (1) can be presented in a simple form: Eq. (2) regardless of the external wrench.

$$\begin{bmatrix} a_{11} & \cdots & a_{1m} \\ \vdots & \ddots & \vdots \\ a_{(m-1)1} & \cdots & a_{(m-1)m} \end{bmatrix} \begin{bmatrix} t_1 \\ \vdots \\ t_m \end{bmatrix} = \mathbf{0} \quad (2)$$

By moving the m column of the first matrix to the right side of the equation, Eq. (2) is deduced as:

$$\begin{bmatrix} a_{11} & \cdots & a_{1(m-1)} \\ \vdots & \ddots & \vdots \\ a_{(m-1)1} & \cdots & a_{(m-1)(m-1)} \end{bmatrix} \begin{bmatrix} t_1 \\ \vdots \\ t_{(m-1)} \end{bmatrix} = -t_m \begin{bmatrix} a_{1m} \\ \vdots \\ a_{(m-1)m} \end{bmatrix} \quad (3)$$

Then, Eq. (3) unveils the available result that tensions can be calculated only if the matrix is not singular by giving one cable tension. Furthermore, the position and orientation is part of the workspace if all cable tensions are positive.

From the point of engineering, the tension range is limited to prevent the looseness of cables and avoid cable breakage as Eq. (4).

$$0 < t_{\min} \leq t_i \leq t_{\max} \quad (i = 1, 2, \dots, m) \quad (4)$$

Combining Eq. (3) with Eq. (4), the workspace and the tensions in arbitrary positions and orientations can be obtained.

5. Quality workspace indices

At first, the usual index to evaluate the workspace quality is to compare the volume of position workspaces.

In order to measure the workspace quality further, Tension Factor (TF) and Global Tension Index (GTI) are proposed by C. B. Pham[17]. TF reflects the tension distribution by the putting minimum tension over the maximum tension. To study the distribution of all cable tensions clearly and analyse the effect of tension distribution, the All Cable Tension Distribution Index

(ACTDI) is defined with the variance of all tensions as following:

$$ACTDI = \sqrt{\frac{\sum_{i=1}^m (t_i - \bar{t})^2}{(m-1)}} \quad (i = 1, 2, \dots, m) \quad (5)$$

where \bar{t} is the average value of tensions. If ACTDI is smaller, the tensions are closer to each other so that the workspace quality is considered better.

Similar to the GTI defined by C. B. Pham, the Global Tension Distribution Index (GTDI) is presented to evaluate the whole workspace quality.

$$GTDI = \frac{\sum_1^{n_1} i(ACTDI \leq 1)}{\sum_1^{n_2} j} \quad (6)$$

where n_1 is the total number of the poses with ACTDI equal to or less than 1, and n_2 is the total number of the poses over the workspace.

6. Workspace quality analysis

In this section, we will make use of ACTDI and GTDI to measure the quality of the workspace with Completely Restrained CDPMs by 7 cables in different configurations.

Given the minimum tension $t_{\min}=1(N)$ and the maximum allowed tension $t_{\max}=20(N)$, the position workspace with tension limitation is obtained based on the approach mentioned above in Fig. 3, and the orientation workspace with tension limitation is shown in Fig. 4.

As shown in Fig.3, all these position workspaces are axisymmetric about the y axis in correspondence with the joint distribution. Specifically, the type 1-6 model position workspace has a broad workspace at $z=0mm$, but shrinks quickly to one point at $z=1000mm$. However, the type 3-4 model position workspace maintains the similar shape as type 1-6 model except for when upside down. As for the type 2-5 model, the largest area of the workspace along the z axis is in the middle. The volume of position workspaces about these configurations is listed in Table 3. The type 3-4 model retains the largest volume of position workspace, whereas the type 1-6 model has the smallest volume.

Type	Volume/m ³
1-6	0.0131
2-5	0.0257
3-4	0.0820

Table 3. Volume of Position Workspace

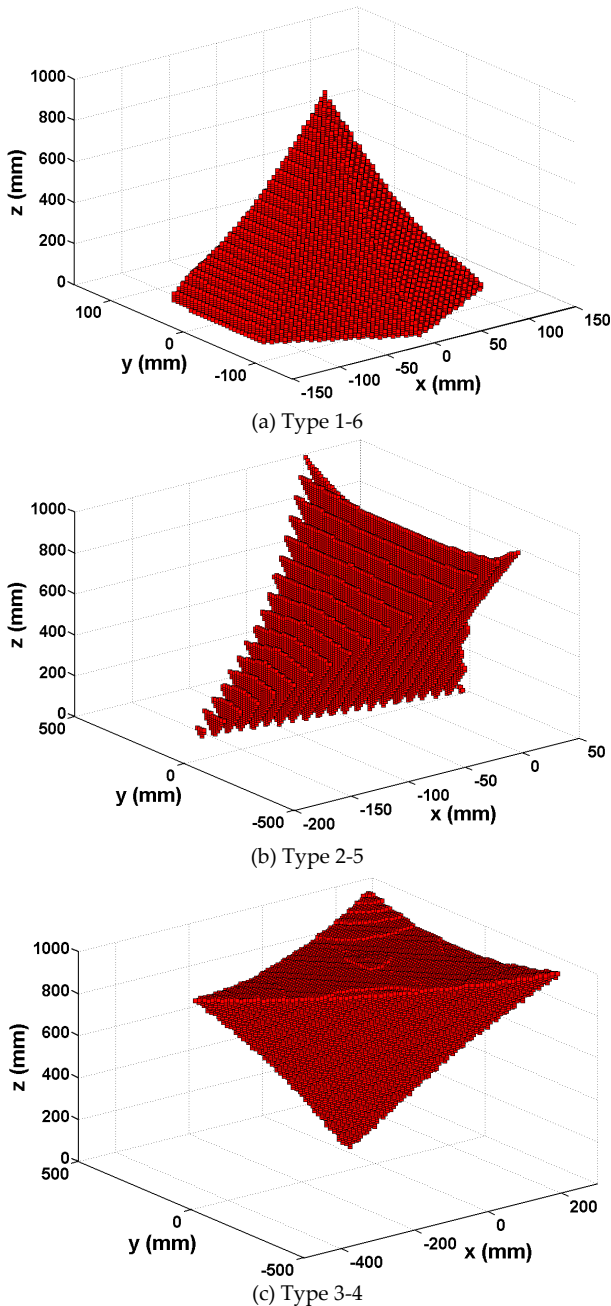


Figure 3. Position Workspace with $\alpha = 0^\circ, \beta = 0^\circ, \gamma = 0^\circ$

In Fig.4, the orientation workspaces with the position ($x=0\text{mm}, y=0\text{mm}, z=500\text{mm}$) are dissimilar from each other where the type 3-4 model has a broader range of rotational angles than the type 1-6 and 2-5 models.

By using ACTDI, the tension distribution is evaluated by sections along x, y and z axes across the position workspace as well as along α, β, γ axes across the orientation workspace. Due to the definition of ACTDI, the tension distribution is more uniform if the index maintains a smaller value. For example, ACTDI in sections of the type 1-6 model is calculated and shown in Fig. 5.

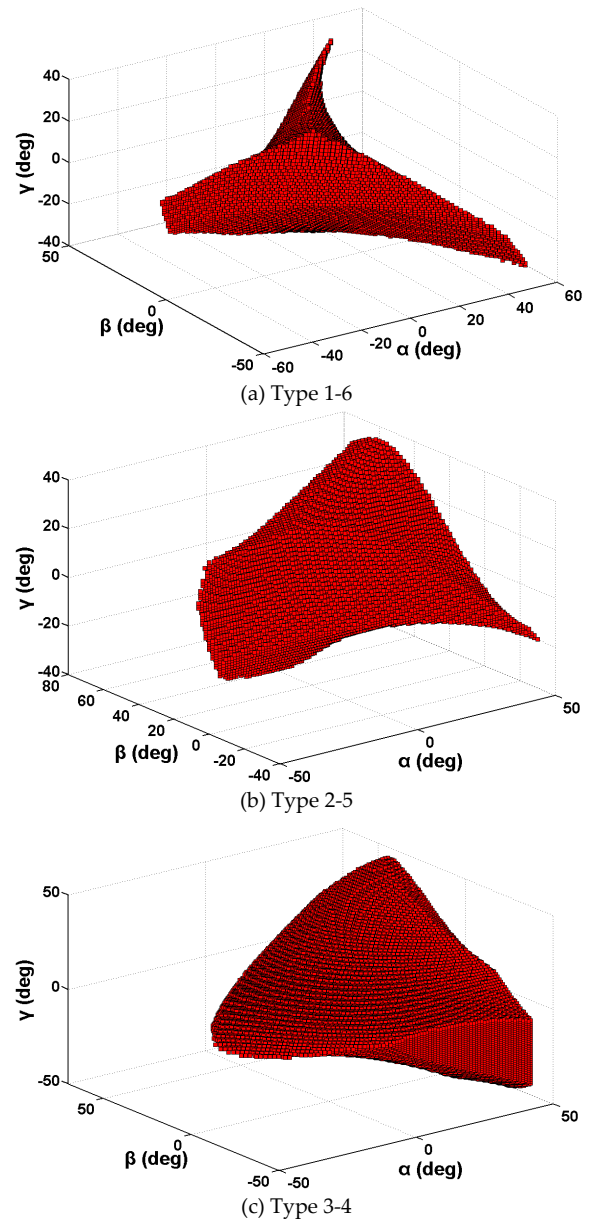


Figure 4. Orientation Workspace with $x = 0(\text{mm}), y = 0(\text{mm}), z = 500(\text{mm})$

As illustrated in Fig. 4, ACTDI in orientation workspaces are discontinuous because of avoiding cable interference. Comparing orientation workspace in Fig. 4, type 2-5 and 3-4 models are better if the key point is to have a large orientation. Thus, the type 2-5 and 3-4 models can be optimized with the joint distribution such that the orientation workspace can expand greatly.

As shown in Fig. 5, the value of ACTDI across both position workspace and orientation workspace increases from the inside to the outside, which denotes that positions around the origin of the lower fixed platform have even tension distributions but the points far away from the origin are more unreasonable in tension distribution. Similarly, ACTDI in the other two type models are depicted in Fig. 6 and Fig. 7.

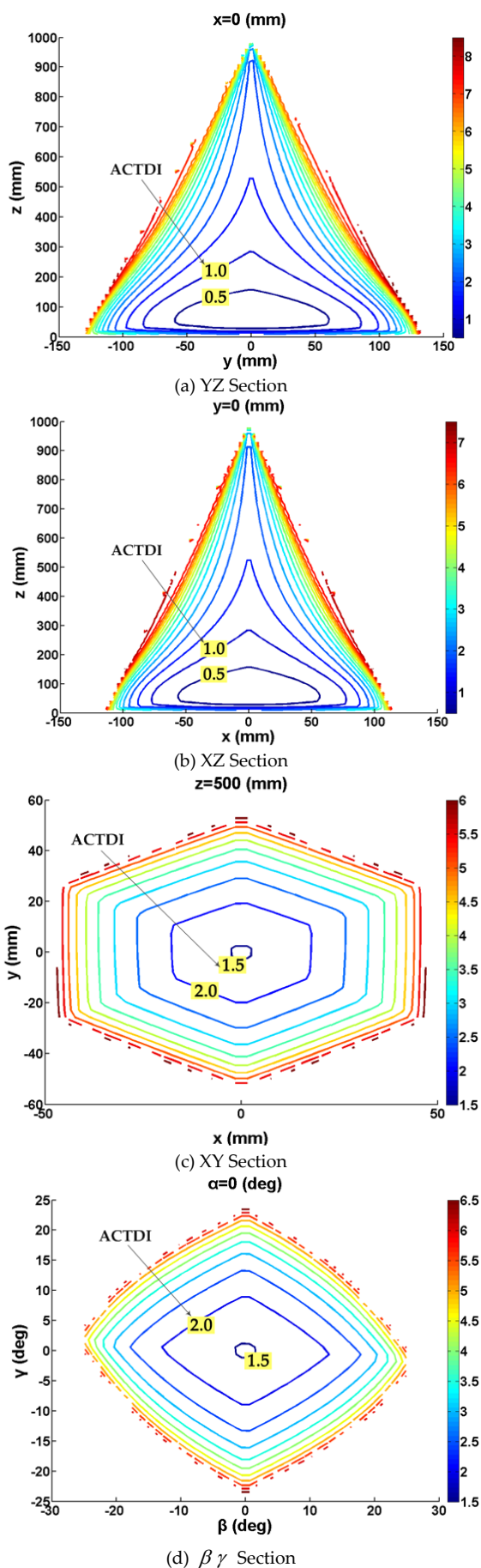


Figure 5. Sections of Type 1-6 Model with ACTDI

By the representation of ACTDI over sections in position workspace, the value is lower near the lower fixed platform than in other positions. Furthermore, the heights with the lowest values of ACTDI are different from each other among the three type models. In the view of ACTDI in sections, the type 3-4 model maintains a better position workspace because ACTDI changes less than other type models.

From the analysis above, ACTDI across various sections of different models is depicted to evaluate the quality of these sections in detail. However, the quality of the whole workspace is more significant to measure and GTDI makes it feasible to evaluate the quality. Based on ACTDI of both position workspace and orientation workspace, GTDI is defined as the positions/orientations with ACTDI equal to/smaller than 1 over the total positions/orientations in the workspace. Moreover, a larger GTDI of a workspace means the tension distribution over the workspace is more uniform than others. Thus, the type 1-6 model maintains a better tension distribution over position workspace by comparing GTDI listed in Table 4 of these models, whereas the type 3-4 model is better in tension distribution over orientation workspace from Table 5.

Type	GTDI
1-6	0.1895
2-5	0.0698
3-4	0.1156

Table 4. GTDI of Position Workspace

Type	GTDI
1-6	0
2-5	0.0115
3-4	0.3536

Table 5. GTDI of Orientation Workspace

According to these indices mentioned above, the volume of position workspace reflects that the type 3-4 model obtains a larger position workspace than other two type models. As for ACTDI across sections, ACTDI over the type 3-4 model changes less significantly so that most of the area over the sections maintains a uniform tension distribution. Finally, GTDI integrates ACTDI over the whole workspace to measure the quality of the workspace. In these three type configurations of completely restrained CDPMs, the results of GTDI denote that the position workspace of the type 1-6 model and the orientation workspace of type 3-4 model are related to more even tensions along all the cables.

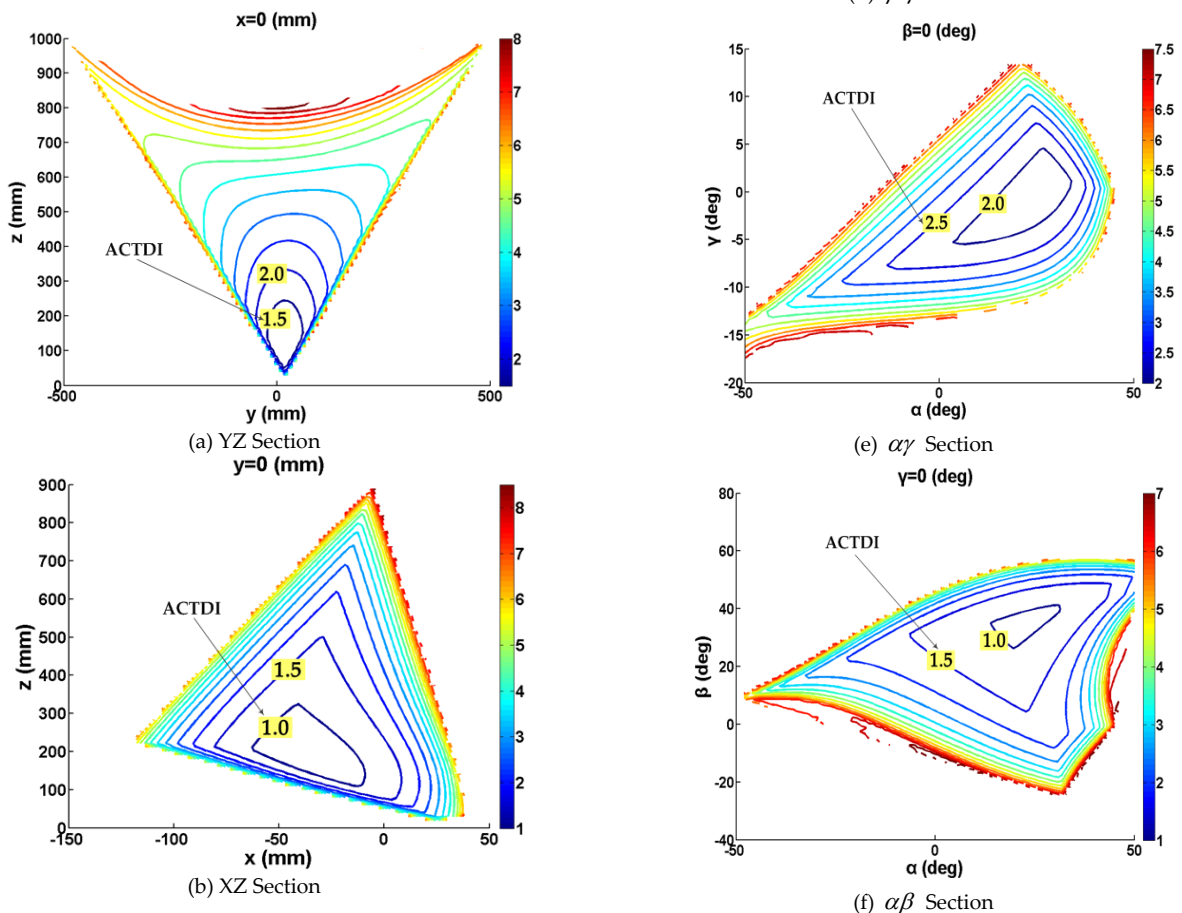
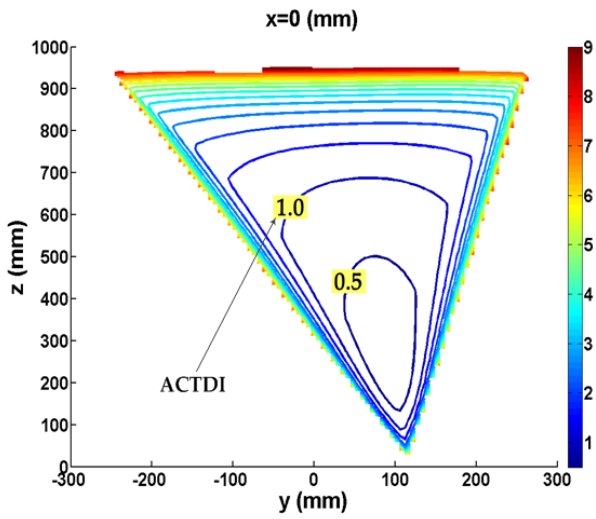
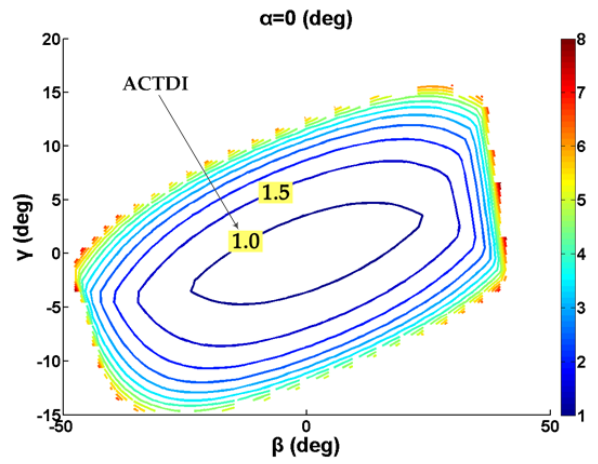


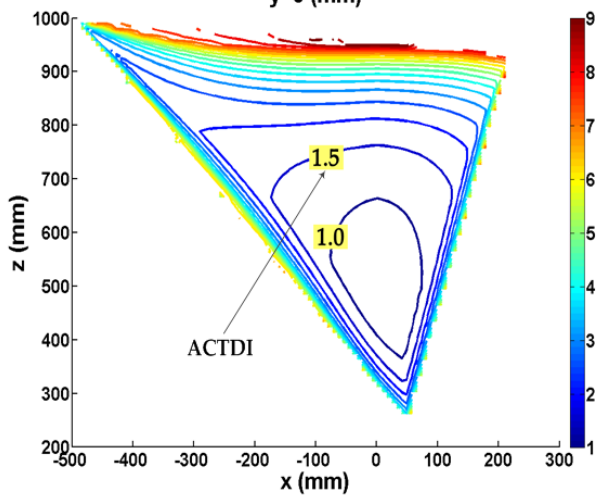
Figure 6. Sections of Type 2-5 Model with ACTDI



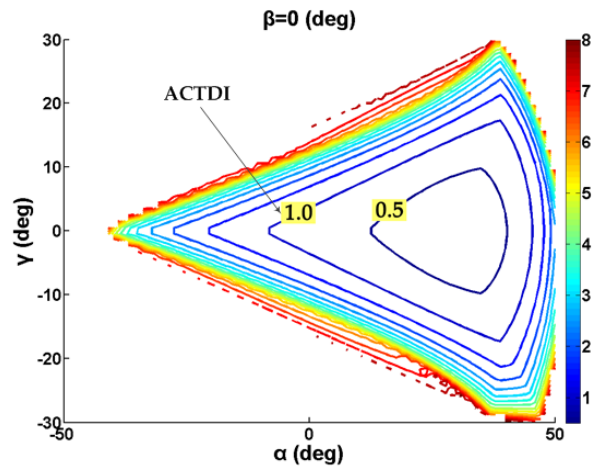
(a) YZ Section
y=0 (mm)



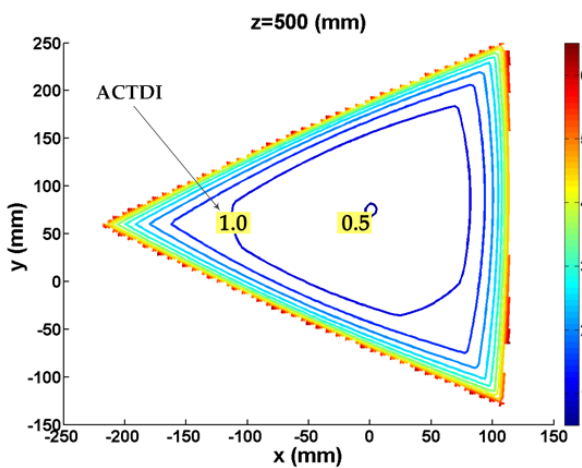
(d) $\beta\gamma$ Section



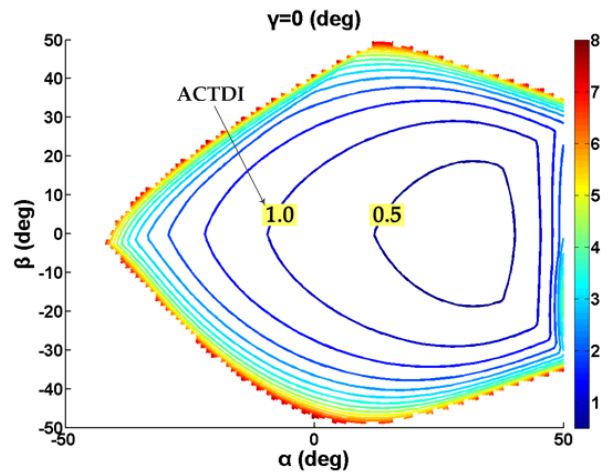
(b) XZ Section



(e) $\alpha\gamma$ Section



(c) XY Section



(f) $\alpha\beta$ Section

Figure 7. Sections of Type 3-4 Model with ACTDI

7. Conclusion

In this paper, the main problem we aim to solve is the evaluation of both the position workspace and the orientation workspace in different configurations of fully restrained CDPMs suspended by 7 cables. Due to the features of cables, the workspace of CDPMs is defined by the tensions along all the cables which satisfy the force-condition with a positive value. From the analysis of configurations of fully restrained CDPMs with 7 cables regardless of gravity, 8 types of cables distribution are found based on the modelling principles. However, the two types with all the cables connected to the moving platform fixed the platform on one side are invalid because they fail to meet the force condition. Considering the symmetry, only three type models are presented for research. In order to evaluate the workspace quality, two new evaluation indices, namely ACTDI and GTDI, are defined with tensions in each cable. By using the approach above, the workspace is found with respect to position and orientation and the corresponding tensions. To this extent, ACTDI over various sections reflects tension distribution. Besides, GTDI has proved that the type 3-4 model maintains a more uniform tension distribution over orientation workspace as well as the type 1-6 model over position workspace. In addition, a much larger position workspace is obtained with the type 3-4 model than with the others.

8. Acknowledgments

This research is sponsored by the National Natural Science Foundation of China (No. 11178012, 50975149), and the National S&T Major Project of China (No. 2011ZX04015-011).

9. References

- [1] C. B. Pham, S. H. Yeo, and G. L. Yang, "Workspace Analysis and Optimal Design of Cable-Driven Planar Parallel Manipulator," in: *Proc. of the 2004 IEEE Inter. Conf. on Robotics, Automation, and Mechatronics*, 2004, pp. 219-224.
- [2] W. B. Lim, G. L. Yang, S. H. Yeo, and S. K. Mustafa, "A generic force-closure analysis algorithm for cable-driven parallel manipulators," in *Mechanism and Machine Theory*, 46, 2011, pp.1265-1275.
- [3] X. Diao, and O. Ma, "A method of verifying force-closure condition for general cable manipulators with seven cables," in *Mechanism and Machine Theory*, 42, 2007, pp. 1563-1576.
- [4] M. Hassan, and A. Khajepour, "Analysis of Bounded Cable Tensions in Cable-Actuated Parallel Manipulators," in *Robotics*, 27, 2011, pp. 891-900.
- [5] M. Agahi, and L. Notash, "Investigation of Force Capability in Planar Wire-Actuated Parallel Manipulators for Wire Failure," in: *13th World Congress in Mechanism and Machine Science*, 2011, pp. 1-10.
- [6] R. Verhoeven, M. Hiller, and S. Tadokoro, "Workspace, stiffness, singularities and classification of tendon-driven Stewart platforms," in: *Proc. of 6th Int. Symp. Adv. Robot Kinematics*, Strobl, Austria, 1998, pp. 105-114.
- [7] G. Yang, S. H. Yeo, and C. B. Pham, "Kinematics and Singularity Analysis of a planar Cable-Driven Parallel Manipulator," in: *Proc. of 2004 IEEE/RSJ Inter. Conf. on intelligent Robots and Systems*, Sendai, Japan, 2004, pp.3835-3840.
- [8] S. Fang, D. Franitza, M. Torlo, F. Bekes, and M. Hiller, "Motion Control of a Tendon-Based Parallel Manipulator Using Optimal Tension Distribution," in *Mechatronics*, 9, 2004, pp. 561-567.
- [9] S. Lahouar, E. Ottaviano, S. Zeghoul, L. Romdhane, and M. Ceccarelli, "Collision free path-planning for cable-driven parallel robots," in *Robotics and Autonomous Systems*, 57, 2009, pp.1083-1093.
- [10] D. McColl, and L. Notash, "Workspace envelope formulation of planar wire-actuated parallel manipulators," in *Transactions of the Canadian Society for Mechanical Engineering*, 33, 2009, pp.547-560.
- [11] M. Couttefarde, and C. M. Gosselin, "Analysis of the Wrench-Closure Workspace of Planar Parallel Cable-Driven Mechanisms," in *Robotics*, 22, 2006, pp.434-445.
- [12] E. Stump, and V. Kumar, "Workspace delineation of cable-actuated parallel manipulators," in: *Proc. of DETC'04 ASME 2004*, Salt Lake City, USA, 2004, pp.1-8.
- [13] X. Q. Tang, and R. Yao, "Dimensional design on the six-cable driven parallel manipulator of FAST," in *ASME Journal of Mechanical Design*, 133, 2011, pp.1-12.
- [14] X. Q. Tang, W. B. Zhu, C. H. Sun, and R. Yao, "Similarity model of feed support system for FAST," in *Experimental Astronomy*, 29, 2011, pp.177-187.
- [15] C. B. Pham, S. H. Yeo, G. L. Yang, M. S. Kurbanhusen, and I. Chen, "Force-closure workspace analysis of cable-driven parallel mechanisms, " in *Mechanism and Machine Theory* , 41, 2006, pp. 53-69.
- [16] D. Lau, and D. Oetomo, "Wrench-Closure Workspace Generation for Cable Driven Parallel Manipulators using a Hybrid Analytical-Numerical Approach, " in *Journal of Mechanical Design*, 133, 2011 : 071004
- [17] C. B. Pham, S. H. Yeo, G. L. Yang, and I. Chen, "Workspace Analysis of fully restrained cable-driven manipulators, " in *Robotics and Autonomous Systems*, 52, 2009, pp. 901-912.

Appendix

Dimensions of the Type 1-6 model (unit: mm)

Position vector	x	y	z
${}^0\mathbf{a}_1$	0	0	1000
${}^0\mathbf{a}_2$	500	0	0
${}^0\mathbf{a}_3$	250	433	0
${}^0\mathbf{a}_4$	-250	433	0
${}^0\mathbf{a}_5$	-500	0	0
${}^0\mathbf{a}_6$	-250	-433	0
${}^0\mathbf{a}_7$	250	-433	0

Position vector	x	y	z
${}^e\mathbf{b}_1$	0	0	0
${}^e\mathbf{b}_2$	130	75	0
${}^e\mathbf{b}_3$	130	75	0
${}^e\mathbf{b}_4$	-130	75	0
${}^e\mathbf{b}_5$	-130	75	0
${}^e\mathbf{b}_6$	0	-150	0
${}^e\mathbf{b}_7$	0	-150	0

Dimensions of the Type 2-5 model (unit: mm)

Position vector	x	y	z
${}^0\mathbf{a}_1$	0	-500	1000
${}^0\mathbf{a}_2$	0	500	1000
${}^0\mathbf{a}_3$	500	0	0
${}^0\mathbf{a}_4$	154.5	475.5	0
${}^0\mathbf{a}_5$	-404.5	293.9	0
${}^0\mathbf{a}_6$	-404.5	-293.9	0
${}^0\mathbf{a}_7$	154.5	-475.5	0

Position vector	x	y	z
${}^e\mathbf{b}_1$	0	0	0
${}^e\mathbf{b}_2$	0	0	0
${}^e\mathbf{b}_3$	130	75	0
${}^e\mathbf{b}_4$	130	75	0
${}^e\mathbf{b}_5$	-130	75	0
${}^e\mathbf{b}_6$	0	-150	0
${}^e\mathbf{b}_7$	0	-150	0

Dimensions of the Type 3-4 model (unit: mm)

Position vector	x	y	z
${}^0\mathbf{a}_1$	250	-433	1000
${}^0\mathbf{a}_2$	250	433	1000
${}^0\mathbf{a}_3$	-500	0	1000
${}^0\mathbf{a}_4$	353.6	353.6	0
${}^0\mathbf{a}_5$	-353.6	353.6	0
${}^0\mathbf{a}_6$	-353.6	-353.6	0
${}^0\mathbf{a}_7$	353.6	-353.6	0

Position vector	x	y	z
${}^e\mathbf{b}_1$	0	0	0
${}^e\mathbf{b}_2$	0	0	0
${}^e\mathbf{b}_3$	0	0	0
${}^e\mathbf{b}_4$	130	75	0
${}^e\mathbf{b}_5$	-130	75	0
${}^e\mathbf{b}_6$	0	-150	0
${}^e\mathbf{b}_7$	0	-150	0